

SeqVLM: Proposal-Guided Multi-View Sequences Reasoning via VLM for Zero-Shot 3D Visual Grounding

Jiawen Lin^{*}

School of Informatics, Xiamen University
Xiamen, Fujian, China
linjiawen@stu.xmu.edu.cn

Wenbin Tan

School of Informatics, Xiamen University
Xiamen, Fujian, China
wbtan@stu.xmu.edu.cn

Shiran Bian^{*}

School of Informatics, Xiamen University
Xiamen, Fujian, China
bianshiran@foxmail.com

Yihang Zhu

School of Computer Science, Nanjing University
Nanjing, Jiangsu, China
zhu_yih@163.com

Yachao Zhang[†]

School of Informatics, Xiamen University
Xiamen, Fujian, China
yachaozhang@xmu.edu.cn

Yuan Xie

School of Computer Science and Technology, East China Normal University
Shanghai, China
yxie@cs.ecnu.edu.cn

Yanyun Qu[†]

Key Laboratory of Multimedia Trusted Perception and Efficient Computing, Ministry of Education of China, Xiamen University
Xiamen, Fujian, China
yyqu@xmu.edu.cn

Abstract

3D Visual Grounding (3DVG) aims to localize objects in 3D scenes using natural language descriptions. Although supervised methods achieve higher accuracy in constrained settings, zero-shot 3DVG holds greater promise for real-world applications since eliminating scene-specific training requirements. However, existing zero-shot methods face challenges of spatial-limited reasoning due to reliance on single-view localization, and contextual omissions or detail degradation. To address these issues, we propose SeqVLM, a novel zero-shot 3DVG framework that leverages multi-view real-world scene images with spatial information for target object reasoning. Specifically, SeqVLM first generates 3D instance proposals via a 3D semantic segmentation network and refines them through semantic filtering, retaining only semantic-relevant candidates. A proposal-guided multi-view projection strategy then projects these candidate proposals onto real scene image sequences, preserving spatial relationships and contextual details in the conversion process of 3D point cloud to images. Furthermore, to mitigate VLM computational overload, we implement a dynamic scheduling mechanism that iteratively processes sequences-query prompts, leveraging VLM's

cross-modal reasoning capabilities to identify textually specified objects. Experiments on the ScanRefer and Nr3D benchmarks demonstrate state-of-the-art performance, achieving Acc@0.25 scores of 55.6% and 53.2%, surpassing previous zero-shot methods by 4.0% and 5.2%, respectively, which advance 3DVG toward greater generalization and real-world applicability. The code is available at <https://github.com/JiawLin/SeqVLM>.

CCS Concepts

• Computing methodologies → Artificial intelligence; Computer vision tasks; Scene understanding.

Keywords

3D Visual Grounding, Multi-View Sequences, Visual-Language Model, Zero-shot Scene Understanding

ACM Reference Format:

Jiawen Lin^{*}, Shiran Bian^{*}, Yihang Zhu, Wenbin Tan, Yachao Zhang[†], Yuan Xie, and Yanyun Qu[†]. 2025. SeqVLM: Proposal-Guided Multi-View Sequences Reasoning via VLM for Zero-Shot 3D Visual Grounding. In *Proceedings of the 33rd ACM International Conference on Multimedia (MM '25)*, October 27–31, 2025, Dublin, Ireland. ACM, New York, NY, USA, 10 pages. <https://doi.org/10.1145/3746027.3754985>

Permission to make digital or hard copies of all or part of this work for personal or classroom use is granted without fee provided that copies are not made or distributed for profit or commercial advantage and that copies bear this notice and the full citation on the first page. Copyrights for components of this work owned by others than the author(s) must be honored. Abstracting with credit is permitted. To copy otherwise, or republish, to post on servers or to redistribute to lists, requires prior specific permission and/or a fee. Request permissions from permissions@acm.org.

MM '25, Dublin, Ireland

© 2025 Copyright held by the owner/author(s). Publication rights licensed to ACM.

ACM ISBN 979-8-4007-2035-2/2025/10

<https://doi.org/10.1145/3746027.3754985>

1 Introduction

3D Visual Grounding (3DVG) is a critical task that aims to establish cross-modal alignment between natural language descriptions and target objects in 3D scenes. Given a 3D scene represented as point

^{*}Jiawen Lin and Shiran Bian contributed equally to this work.

[†]Yanyun Qu and Yachao Zhang are corresponding authors.

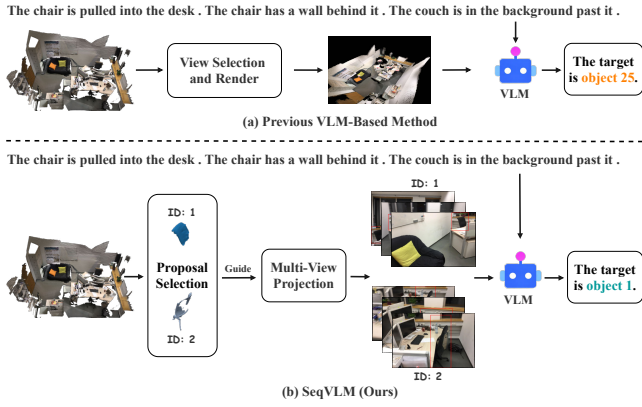


Figure 1: Comparative overview of previous VLM-based methods and SeqVLM. (a) Previous VLM-Based Method for 3DVG use single-view images for localization. (b) SeqVLM integrates proposal-guided with multi-view real-image projection for accurate 3DVG.

clouds and a semantically rich textual query (e.g., *"the red chair near the window"*), the task requires a model to precisely infer the 3D bounding box coordinates of the referred object. This technology holds significant application value in intelligent human-robot interaction [24, 27], autonomous driving environmental perception [58, 61], and AR/VR systems [40, 57].

Current approaches predominantly rely on fully supervised paradigms [6, 14, 16, 29, 34, 46, 51, 54], achieving localization through training on fixed text-scene paired datasets. Although these methods attain high accuracy in closed datasets, they suffer from two limitations: (1) High annotation costs for 3D bounding boxes restrict training data scale, hindering generalization to real-world scene complexity [15, 17, 25]; (2) Strict dependence on annotated data impedes adaptation to open-vocabulary scenarios [10, 39].

Zero-shot and open-vocabulary learning provide promising directions to address these limitations [24, 32, 48, 50, 52]. Zero-shot learning enables models to localize unseen objects without training, while open-vocabulary learning focuses on constructing models capable of processing arbitrary vocabulary. The integration of these paradigms enhances model generalization and broadens application scenarios. Concurrently, capitalizing on the profound semantic and scene-level understanding of large language models (LLMs) [8, 13, 44, 45, 55] and visual-language models (VLMs) [9, 19, 33, 60], researchers are developing zero-shot 3D visual grounding frameworks to tackle open-vocabulary challenges.

Existing zero-shot 3DVG methods primarily fall into two categories: LLM-based and VLM-based methods. LLM-based methods [50, 52] convert textual descriptions into structured programmatic instructions via LLMs, then execute code-based object retrieval in point cloud space. While these methods leveraging LLMs' superior semantic comprehension to parse complex language structures, they struggle with sparse point clouds' inherent limitations in capturing color/texture cues and reasoning about intricate spatial relationships. Conversely, as shown in Figure 1(a), previous VLM-based methods [24, 48] enhance 3D visual grounding by integrating 2D

visual features to identify objects in images that best match text descriptions. However, their reliance on single-view renderings may introduce cascading limitations. The absence of 3D geometric constraints leads to spatial biases that misalign 2D projections with 3D coordinates, while single-view perspectives inherently fail to resolve occlusions or capture multi-object contextual relationships. These issues are further compounded by gaps between rendered and real-world imagery, such as chromatic aberrations, texture simplification, and occlusion [5, 49], which systematically degrade the VLMs' ability to reason about fine-grained visual-textual correspondences [23, 26, 56]. Collectively, these limitations highlight the critical need for geometrically consistent, multi-view fusion strategies in real-world 3D grounding scenarios.

To address these challenges, we propose SeqVLM, a novel framework that enhances cross-modal alignment for zero-shot 3DVG by leveraging multi-view real-world image sequences. SeqVLM integrates 3D point clouds, multi-view images, and natural language descriptions, utilizing VLM for cross-modal alignment to achieve precise 3D object localization. The overall pipeline of SeqVLM is illustrated in Figure 1(b).

Specifically, our framework uses a 3D semantic segmentation network to extract object proposals from 3D point cloud scenes. To improve accuracy and efficiency, irrelevant proposals are filtered through semantic alignment with the target object category described in the input, retaining only those that match semantically with the specified category. The refined proposals are then projected onto real-world image sequences to generate context-aware regions with multi-view consistency, preserving spatial relationships and details. To address the constraints imposed by VLM input length, we introduce an iterative reasoning mechanism that dynamically schedules inference, optimizing both inference efficiency and localization accuracy. Compared to existing approaches, SeqVLM has two main advantages: First, proposal-guided projection strategy effectively maintains 3D geometric attributes and environmental context, significantly reducing localization errors. Second, by leveraging multi-view real images, SeqVLM enhances spatial understanding and contextual awareness, thereby enhancing the cross-modal alignment of VLMs. These innovations enable robust zero-shot 3DVG in complex environments.

SeqVLM achieves absolute improvements of 4.0% and 5.2% in Acc@0.25 on ScanRefer [6] and Nr3D [1], respectively, outperforming existing zero-shot methods. Notably, its performance rivals fully supervised approaches on certain metrics.

Overall, our contributions are summarized as follows:

- We propose SeqVLM, a novel framework that integrates 3D geometric features with 2D visual cues via proposal-guided multi-view projection, enabling accurate cross-modal localization in zero-shot settings.
- We develop a proposal-guided multi-view projection strategy, which aligns objects semantically relevant to textual descriptions with real-scene images across multiple viewpoints. This ensures precise projection positioning while preserving contextual and detailed scene information.
- We design an iterative reasoning mechanism to address VLM failure in multi-candidate scenarios through dynamic computational scheduling.

- We conduct extensive experiments on the ScanRefer and Nr3D datasets, demonstrating the effectiveness of our framework and setting new state-of-the-art performance in zero-shot 3D visual grounding.

2 Related Work

2.1 Supervised 3DVG

Current research in 3D visual grounding predominantly adopts supervised learning paradigms, achieving cross-modal alignment through training on annotated datasets. Existing methodologies can be categorized into two technical frameworks: two-stage and single-stage approaches.

Two-stage methods [1, 6, 7, 18, 58] employ a "detect-then-match" cascade architecture. The first stage generates candidate object proposals via 3D object detection or instance segmentation [20, 28, 41], while the second stage constructs cross-modal alignment modules to refine language-query matching with candidate region features and optimize bounding boxes [4, 29]. In contrast, single-stage methods [34, 43, 46] utilize end-to-end architectures to jointly model 3D point clouds and textual features, achieving dense regression predictions of target locations. Notably, SAT [51] pioneers the integration of 2D image semantics as auxiliary supervision during training, enhancing joint representation learning between 3D point clouds and language via cross-modal alignment, thereby significantly improving localization accuracy. Despite remarkable progress, supervised approaches face two critical bottlenecks: (1) High annotation costs for 3D data restrict dataset scalability, limiting coverage of complex real-world scenarios; (2) Model generalization is constrained by closed-vocabulary settings, hindering adaptation to open-world localization of unseen objects.

2.2 Zero-Shot 3DVG

Zero-shot methods aim to overcome the annotation dependency of supervised paradigms by leveraging the cross-modal reasoning capabilities of pretrained large models, primarily divided into Large Language Model (LLM)-based and Visual-Language Model (VLM)-based methods.

LLM-based methods [50, 52] parse natural language queries through linguistic models, converting them into structured semantic elements or executable program instructions. These methods combine geometric reasoning with commonsense knowledge for zero-shot localization. While effective in handling complex semantic inference, they exhibit limitations in exploiting 3D scene contextual information and effectively integrating fine-grained visual features.

VLM-based methods [24, 48], leverage the multimodal alignment capabilities of visual-language models, enabling the integration of visual and textual information for enhanced scene understanding. VLM-Grounder [48] proposes dynamically stitching multi-view 2D image sequences, utilizing VLM's open-vocabulary reasoning to infer 2D object masks, followed by multi-view projection and morphological processing for 3D bounding box reconstruction. See-Ground [24] further introduces dynamically rendered 2D images with spatially enriched 3D text descriptions, utilizing a Perspective Adaptation Module for query-aligned views and a Fusion Alignment

Module to improve object localization. Despite improved scene context utilization, these methods remain constrained by some key factors: (1) Geometric misalignment errors arising from improper projection methodologies; (2) Loss of spatial information related to viewpoint-specific cues due to single-view constraints; (3) Visual feature distortion due to domain gaps between rendered images and real-world scenes.

3 Methodology

3.1 Task Definition

We consider a 3D scene represented by a colored point cloud $\mathbf{P} \in \mathbb{R}^{N \times 6}$, where each point is characterized by XYZ coordinates and RGB color attributes, along with an image list captured from various viewpoints in real-world scenes, and a textual description T specifying the target object O^* . Our task focuses on zero-shot 3DVG that localizes the O^* in 3D space without requiring scene-specific training or fine-tuning. The image list can be obtained through various sensors including RGB-D sensors with structured light scanners [30, 38], dense SLAM systems [11, 12, 22] or Time-of-Flight (ToF) sensors [35, 47].

3.2 Overview

The framework of SeqVLM is illustrated in Figure 2. Given a point cloud scene \mathbf{P} , a 3D semantic segmentation network is first employed to perform instance segmentation, followed by confidence-based filtering to extract object categories and corresponding mask features. Then, LLM parses the textual description T to identify the target object category, denoted as C^* . This category, along with the filtered object categories, is embedded using a text encoder. Based on the cosine similarity matching, a proposal list O is generated, containing n proposals that are semantically related to the target category. For each proposal $O_i \in O$, all scene images from \mathbf{P} are sampled to form an image list I_i . Multi-view projection is applied to annotate the region corresponding to O_i in each image within I_i . The top n_{frame} images with the largest projected areas are then stitched, generating a vertical image sequence S_i as the 2D visual representation of O_i . Finally, using an iterative reasoning mechanism, the proposal sequences $\mathcal{S} = [S_1, S_2, \dots, S_k]$, together with the textual description T , are fed into the VLM for cross-modal reasoning to identify the target object O^* . By deeply integrating multimodal information, SeqVLM significantly enhances localization accuracy and robustness, offering an effective solution for zero-shot object localization in complex 3D scenes.

3.3 Proposal Selection Module

We propose to employ a text-driven semantic filtering mechanism to refine proposals whose categories are consistent with the target object. Specifically, the module processes the point cloud scene \mathbf{P} using a 3D semantic segmentation network Φ , and retain only those instances with confidence scores exceeding a predefined threshold θ :

$$\Phi(\mathbf{P}) = \{M_i \mid \sigma(M_i) \geq \theta\}_{i=1}^m, \quad (1)$$

where M_i and $\sigma(\cdot)$ denote the instance mask features and confidence function, respectively. The adoption of threshold filtering effectively eliminates the unreliable segmentation result.

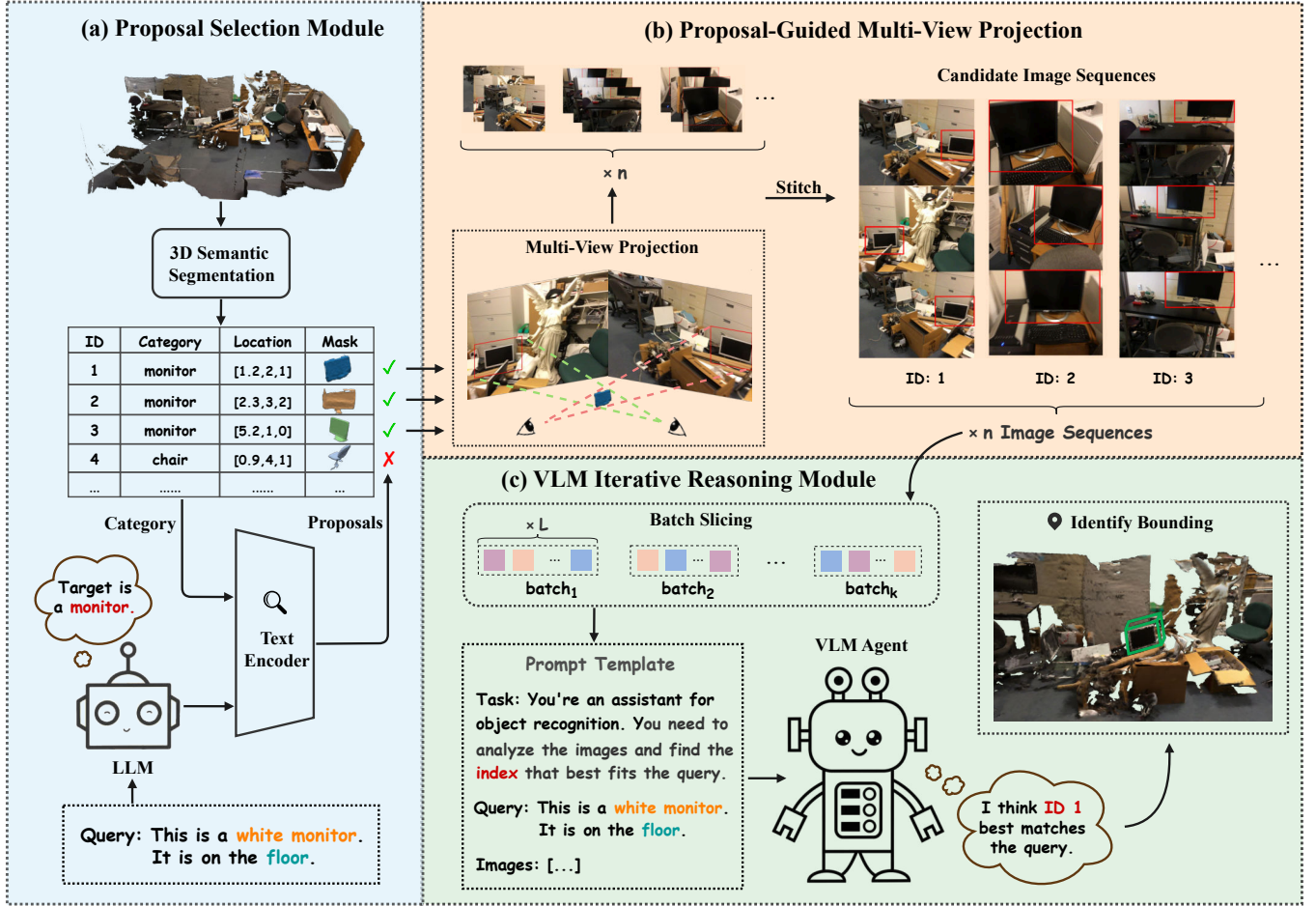


Figure 2: Overview of SeqVLM. Given a 3D scene and a textual query, SeqVLM localizes the target object through a structured pipeline comprising three key modules. First, the Proposal Selection Module employs a 3D semantic segmentation network combined with semantic filtering to extract candidate proposals aligned with the query. Next, the Proposal-Guided Multi-View Projection Module projects these candidates onto optimally selected 2D views, incorporating multi-view stitching to preserve spatial and contextual details. Finally, the VLM Iterative Reasoning Module iteratively refines the search space via a dynamic reasoning mechanism to identify the most probable target. The final selection is then mapped back to its bounding box, ensuring robust localization in complex environments.

Following the dynamic vocabulary mapping in ZSVG3D [52], a structured Object Profile Table(\mathcal{OPT}) can be constructed as:

$$\mathcal{OPT} = \{(ID_i, C_i, BBox_i, M_i)\}_{i=1}^m, \quad (2)$$

where C_i represents the object category and $BBox_i$ corresponds to the 3D bounding box. Then the text encoder is applied to compute the embedding of proposal category C_i and the T_{target} generated by LLM:

$$\begin{aligned} E_t &= f_{text}(T_{target}), \\ E_c^{(i)} &= f_{text}(C_i), \end{aligned} \quad (3)$$

where $f_{text}(\cdot)$ is the text encoder, and the cosine similarity is computed as:

$$\zeta_i = \frac{E_t \cdot E_c^{(i)}}{\|E_t\| \cdot \|E_c^{(i)}\|}. \quad (4)$$

The target object category is determined by the maximum similarity, which then defines the proposal set O as:

$$C^* = \arg \max_{C_i \in \mathcal{OPT}} \zeta_i, \quad (5)$$

$$O = \{M_i \mid C_i = C^*\}_{i=1}^n. \quad (6)$$

This optimization retains only proposals that share the same category as the target, significantly reducing computational complexity in VLM reasoning.

3.4 Proposal-Guided Multi-View Projection

Since VLM cannot process 3D scenes properly, we propose a multi-view projection method that transforms 3D point clouds into 2D images to adapt to VLM. However, in previous works, VLM-Grounder

[48] directly maps 2D detection results to 3D space without considering geometric constraints, and SeeGround [24] relies on restricted single-view rendering, resulting in inadequate spatial understanding and detail loss. Both approaches lack the full utilization of proposal-guided images. To address these limitations, our multi-view projection method is guided by proposals to preserve the context of objects.

Proposal-Guided Projection. For one point belonging to a proposal, its world coordinate can be defined as $P_w = [x_w, y_w, z_w]$, which can be projected into the camera coordinate system of the corresponding view via the homogeneous transformation matrix $T_{wc} \in \mathbb{R}^{4 \times 4}$:

$$P_c = T_{wc} \cdot [x_w, y_w, z_w, 1]^T = [x_c, y_c, z_c, 1]^T. \quad (7)$$

The pixel coordinates (u, v) in the view image are then computed using the intrinsic matrix $\mathbf{K} = \begin{bmatrix} f_x & 0 & c_x \\ 0 & f_y & c_y \\ 0 & 0 & 1 \end{bmatrix}$:

$$u = \frac{x_c \cdot f_x}{z_c} + c_x, \quad v = \frac{y_c \cdot f_y}{z_c} + c_y. \quad (8)$$

To ensure projection validity, we introduce a depth consistency verification:

$$\left| \frac{D(u, v) - z_c}{D(u, v)} \right| \leq \tau, \quad (9)$$

where $D(u, v)$ denotes the depth measurement at (u, v) in the view image, and τ serves as the visibility threshold. If P_w satisfies the consistency after transformation, it is considered valid and visible in the corresponding view.

Multi-View Sequence Generation. For each proposal $M_i \in \mathcal{O}$, which contains a set of point cloud coordinates, we optimize viewpoint selection by quantifying the projected area. The top n_{frame} images with the largest projected areas are selected from the sampled image set \mathcal{I}_i , forming the pixel projection set $\mathcal{P}_i = \{p_i^1, p_i^2, \dots, p_i^{n_{frame}}\}$, where each element represents the pixel projection set of M_i from a certain viewpoint.

During the image stitching phase, each pixel set $p_i^j \in \mathcal{P}_i$ is analyzed to extract its minimum bounding rectangle in the view image:

$$\mathcal{R} = [u_{\min}, v_{\min}, u_{\max}, v_{\max}], \quad (u, v) \in p_i^j, \quad (10)$$

which represents the 2D bounding box of the proposal. To preserve the image details of the object within the bounding box, the box is expanded by the same proportion α along both the width and height directions, and is then highlighted by a distinct 3-pixel-wide red rectangular annotation.

After that, n_{frame} annotated images are vertically concatenated to generate an enhanced image sequence S_i . This process avoids the location deviation during grounding, and enriches spatial relationships and contextual details of object through multiple viewpoints, which are essential for robust 3D scene understanding by VLM.

3.5 VLM Iterative Reasoning Module

We propose an iterative reasoning mechanism to address the sensitivity of VLM to input length in zero-shot 3DVG tasks. Existing works [42, 48, 59] indicate that there is a trade-off between computational load and reasoning accuracy when VLM analyzes a large

number of high-resolution images. If we input all image sequences of \mathcal{S} in a single round of dialogue, it may overload the VLM, degrade performance, or even cause response timeouts. Therefore, we slice the image sequences \mathcal{S} into batches, allowing VLM to optimize the set of proposals over rounds, thus achieving precise localization of the target object.

Algorithm 1 Iterative Reasoning Mechanism

```

Input: Image sequences  $\mathcal{S} = \{S_1, S_2, \dots, S_n\}$ ; Query text  $T$ ; Batch size threshold  $L$  for VLM.
Output: Index of the target object
1: function PREDICT( $\mathcal{S}, T, L$ )
2:    $Q \leftarrow \mathcal{S}$ 
3:   while  $|Q| > 1$  do
4:      $\mathcal{B} \leftarrow \text{SLICE}(Q, L)$  ▷ Slice  $Q$  to batches
5:      $Q \leftarrow []$  ▷ Reset for next round
6:     for each  $B_i$  in  $\mathcal{B}$  do
7:        $prompt \leftarrow \text{CONSTRUCTPROMPT}(T, B_i)$ 
8:        $index \leftarrow \text{VLMSELECT}(prompt)$ 
9:       if  $index \neq \text{None}$  then
10:         $Q \leftarrow Q \cup \mathcal{S}[index]$ 
11:      end if
12:    end for
13:  end while
14:  if  $Q == \emptyset$  then
15:    return None
16:  end if
17:  return  $Q[0].index$ 
18: end function

```

The details of the mechanism are illustrated in Algorithm 1. In this algorithm, the variable Q is defined to dynamically maintain the image sequences that are to be analyzed. Before the iteration process begins, Q will be sliced into batches $\mathcal{B} = \{B_1, B_2, \dots, B_q\}$ with a maximum batch size L . Subsequently, each batch is combined with the textual description T to form the input prompt for the VLM. If the VLM identifies a unique image sequence $S^* \in B_i$ that best matches T , S^* will be reinserted to Q ; otherwise, B_i will be discarded.

After each reasoning step, the algorithm checks the state of Q . The iteration will stop only when $|Q|$ is less than or equal to one. Finally, if only one image sequence remains in Q , its corresponding index is selected as the final result. This mechanism circumvents the limitations of VLM in long-sequence reasoning by gradually reducing the search space.

For 3D localization, the bounding box of selected proposal can be retrieved from the Object Profile Table (\mathcal{OPT}), completing the end-to-end 3DVG pipeline.

4 Experiments

4.1 Experimental Settings

Datasets. We evaluate our framework on two established 3D visual grounding benchmarks: ScanRefer[6] and Nr3D[1]. ScanRefer, constructed from ScanNet, comprises 51,583 natural language descriptions paired with 11,046 objects across 800 indoor scenes, emphasizing fine-grained alignment between linguistic expressions

Table 1: Comparative results on ScanRefer. Evaluates 3D visual grounding by scene type: Unique (target is the sole instance of its class) and Multiple (contains same-class distractors).

Method	Source	Modality	Unique		Multiple		Overall	
			Acc@0.25	Acc@0.5	Acc@0.25	Acc@0.5	Acc@0.25	Acc@0.5
Fully-Supervised Methods								
ScanRefer[6]	ECCV20	3D	67.64	46.19	32.06	21.26	38.97	26.10
TGNN[14]	AAAI21	3D	68.61	56.80	29.84	23.18	37.37	29.70
SAT[51]	ICCV21	3D+2D	73.21	50.83	37.64	25.16	44.54	30.14
MVT[16]	CVPR22	3D+2D	77.67	66.45	31.92	25.26	40.80	33.26
3D-SPS[29]	CVPR22	3D+2D	84.12	66.72	40.32	29.82	48.82	36.98
EDA[46]	CVPR23	3D	85.76	68.57	49.13	37.64	54.59	42.26
3DVLP[54]	CVPR23	3D+2D	84.23	64.61	43.51	33.41	51.41	39.46
MCLN[34]	ECCV24	3D	86.89	72.73	51.96	40.76	57.17	45.53
Zero-Shot Methods								
LERF [21]	ICCV23	3D+2D	-	-	-	-	4.8	0.9
OpenScene [32]	CVPR23	3D+2D	20.1	13.1	11.1	4.4	13.2	6.5
LLM-Grounder [50]	ICRA24	3D	-	-	-	-	17.1	5.3
ZS3DVG [52]	CVPR24	3D+2D	63.8	58.4	27.7	24.6	36.4	32.7
VLM-Grounder[48]	CoRL24	2D	66.0	29.8	48.3	33.5	51.6	32.8
SeeGround[24]	CVPR25	3D+2D	75.7	68.9	34.0	30.0	44.1	39.4
SeqVLM	-	3D+2D	77.3(+1.6)	72.7(+3.8)	47.8	41.3(+7.8)	55.6(+4.0)	49.6(+10.2)

Table 2: Comparative results on Nr3D. Evaluates via Easy (single distractor) vs. Hard (multiple distractors) queries and View-Dependent (requires specific viewpoints) vs. View-Independent scenarios.

Method	Easy	Hard	Dep.	Indep.	Overall
Fully-Supervised Methods					
ReferIt3D[1]	43.6	37.9	32.5	37.1	35.6
TGNN[14]	44.2	30.6	35.8	38.0	37.3
InstanceRefer[53]	46.0	31.8	34.5	41.9	38.8
3DVG-Trans[58]	48.5	34.8	34.8	43.7	40.8
SAT[51]	56.3	42.4	46.9	50.4	49.2
EDA[46]	58.2	46.1	50.2	53.1	52.1
MCLN[34]	-	-	-	-	59.8
Zero-Shot Methods					
ZS3DVG[52]	46.5	31.7	36.8	40.0	39.0
SeeGround[24]	54.5	38.3	42.3	48.2	46.1
VLM-Grounder[48]	55.2	39.5	45.8	49.4	48.0
SeqVLM	58.1	47.4	51.0	54.5	53.2

and 3D object localization through attribute and spatial-relation

reasoning. The dataset is divided into Unique and Multiple subsets: Unique targets objects uniquely identifiable by intrinsic attributes, while Multiple requires disambiguation among multiple instances of the same category using spatial relations. Nr3D contains 41,503 descriptions for 7,189 objects across 1,448 scenes, prioritizing viewpoint-dependent language diversity in real-world contexts. Its evaluation categorizes references into Easy and Hard subsets based on the necessity of implicit contextual reasoning, as well as View-Dependent and View-Independent subsets to assess robustness to observer perspectives.

Implementation Details. Experiments were conducted on a TITAN RTX GPU using Doubao-1.5-pro[3] as the LLM for semantic-guided proposal selection and Doubao-1.5-vision-pro[3] as the VLM for multimodal reasoning. We employ Mask3D [37] as the 3D semantic segmentation network, applying a confidence threshold of 0.2 to filter low-quality segmentation masks. Semantic matching is performed using the CLIP-ViT-Base-Patch16 text encoder [36]. Scene image sequences are segmented into 20-frame intervals for viewpoint sampling, with each candidate object projected across five optimized viewpoints validated through depth consistency checks (visibility threshold is 0.25). We set the bounding region expansion parameter α to 0.25. The VLM processes candidates iteratively through an iterative reasoning mechanism with a batch size limit of four. Due to the high computational cost of VLM-based models, we follow the standardized protocol of VLM-Grounder

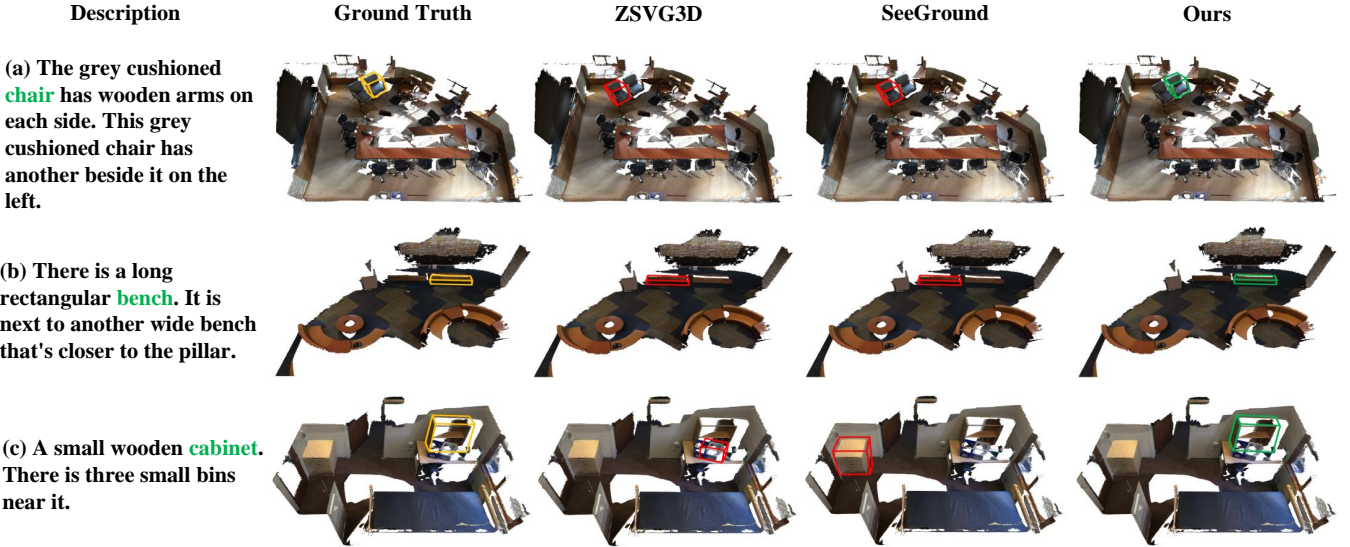


Figure 3: Qualitative results of 3D visual grounding on ScanRefer[6] dataset. Rendered images of 3D scans are presented, including the ground-truth (yellow), incorrectly identified objects (red), and correctly identified objects (green).

[48] for fair evaluation and reproducibility, testing on 250 validation samples per benchmark dataset, matching previous evaluation conditions.

4.2 Quantitative Results

ScanRefer. SeqVLM establishes a new state-of-the-art in zero-shot 3D visual grounding, as demonstrated by the comprehensive comparisons in Table 1, while maintaining competitive performance relative to fully-supervised methods. Specifically, SeqVLM achieves 55.6% Acc@0.25 and 49.6% Acc@0.5 on the overall benchmark, outperforming previous state-of-the-art zero-shot methods, VLM-Grounder[48] and SeeGround[24], by +4.0% and +10.2%, respectively. In single-object scenarios (Unique subset), SeqVLM surpasses prior approaches with gains of 1.6% and 3.8% in Acc@0.25 and Acc@0.5, respectively, highlighting its superior localization accuracy. For multi-object scenarios (Multiple subset), while Acc@0.25 marginally lags behind VLM-Grounder, our method achieves the highest Acc@0.5 performance (+7.8%), demonstrating enhanced fine-grained localization capabilities. Notably, the framework exhibits competitive results against fully-supervised baselines while maintaining strong generalization across diverse 3D visual grounding tasks. These results validate the effectiveness of the proposed method and underscore its potential for practical applications requiring robust 3D spatial reasoning.

Nr3D. As shown in Table 2, SeqVLM attains an overall accuracy of 53.2% on the Nr3D dataset, exceeding prior state-of-the-art zero-shot methods by 5.2%. Our method exhibits robust performance across varying scenario complexities, achieving 58.1% (+2.9%) and 47.4% (+7.9%) accuracy in the "Easy" and "Hard" subsets, respectively. Equally notable is its performance in view-dependent and view-independent scenarios, with accuracies of 51.0% (+5.2%) and 54.5% (+5.1%), illustrating its effective handling of perspective-dependent variations.

The gray padded chair on rollers is the only rolling chair at the table.

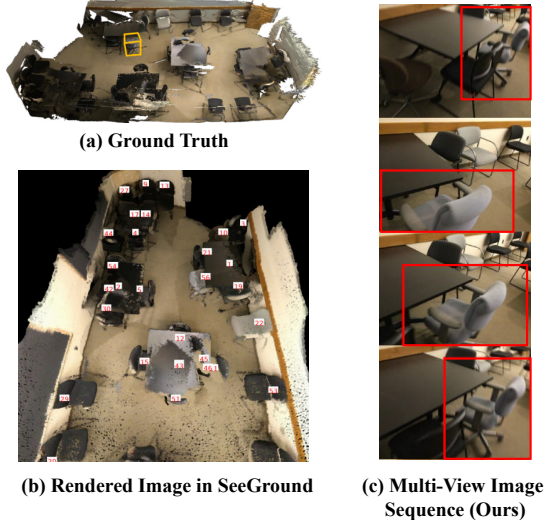


Figure 4: Comparative visualization of single-view rendering and multi-view sequence.

4.3 Qualitative Results

Figure 3 presents the qualitative 3D visual grounding results of ZSVG3D[52], SeeGround [24], and SeqVLM on the ScanRefer [6] dataset. Cases (a–c) demonstrate the superior localization capability of our model, even in complex environments with challenging textual descriptions. For instance, in case (a), our model accurately identifies the target chair despite multiple chairs being present in the scene. In contrast, both baseline methods exhibit lower localization accuracy, with ZSVG3D occasionally misclassifying object

categories (e.g., identifying bins instead of cabinets in case (c)). These qualitative results underscore the efficacy of our approach in enhancing grounding precision and robustness.

Figure 4 contrasts the visual inputs provided to VLM by SeeGround [24] and our method. The ground-truth (a) depicts “*the gray padded chair on rollers. it is the only rolling chair at the table.*” However, SeeGround’s single-view rendering (b) occludes these distinguishing features due to viewpoint constraints, resulting in misidentification. In contrast, our multi-view sequence (c) integrates complementary perspectives, resolving occlusions and clearly revealing the wheels. This visual evidence directly accounts for the accurate localization of our method, demonstrating that multi-view fusion mitigates single-view ambiguities inherent in real-world 3D grounding tasks.

4.4 Ablation Studies

Component Ablation. To evaluate the contribution of core components in our framework, comprehensive ablation studies are conducted on the ScanRefer benchmark as shown in Table 3. The baseline model achieves merely 2.4% accuracy under the Acc@0.5 metric, highlighting the inherent complexity of zero-shot 3D visual grounding. Introducing the Proposal Selection Module significantly improves performance to 43.2% by filtering semantically relevant candidates through text-driven category alignment, whereas standalone implementations of the Multi-View Projection technique or Iterative Reasoning mechanism yield limited gains of 2.0% and 10.0% respectively. The complete framework integrating all components attains 49.6% accuracy, demonstrating substantial synergistic effects through the combination of semantic-aware multi-view 2D visual representations and iterative candidate refinement. This progression underscores the indispensability of each module, particularly the Proposal Selection Module which contributes the most critical performance leap by bridging 3D segmentation with language semantics.

Table 3: Ablation study on different components in our framework on ScanRefer.

Config	Baseline	PSM ¹	MVP ²	IRM ³	Acc@0.5
1	✓				2.4
2	✓	✓			43.2
3	✓		✓		2.0
4	✓			✓	10.0
5	✓	✓	✓		44.4
6	✓		✓	✓	10.4
7	✓	✓		✓	46.0
8	✓	✓	✓	✓	49.6

¹ PSM: Proposal Selection Module.

² MVP: Multi-View Projection.

³ IRM: Iterative Reasoning Mechanism.

VLM Selection. We evaluate the influence of different VLMs on grounding performance and cost. As shown in Table 4, GPT-4[31] achieves 44.0 Acc@0.5 with moderate token usage (1,684k) and cost (2.2\$), while Qwen-vl-max[2] improves accuracy to 46.0 at a lower

Table 4: VLM Performance and Cost .

VLM	Tokens	Cost	Acc@0.5
GPT-4	1,684k	2.2\$	44.0
Qwen-vl-max	1,886k	0.8\$	46.0
Douba-1.5-vision-pro	7,097k	2.9\$	49.6

Table 5: Cross-Method performance comparison under controlled VLM settings.

Method	LLM/VLM	Acc@0.5
VLM-Grounder	GPT-4	32.8
SeqVLM	GPT-4	44.0
ZSVG	Douba-1.5-vision-pro	29.2
SeeGround	Douba-1.5-vision-pro	40.0
SeqVLM	Douba-1.5-vision-pro	49.6

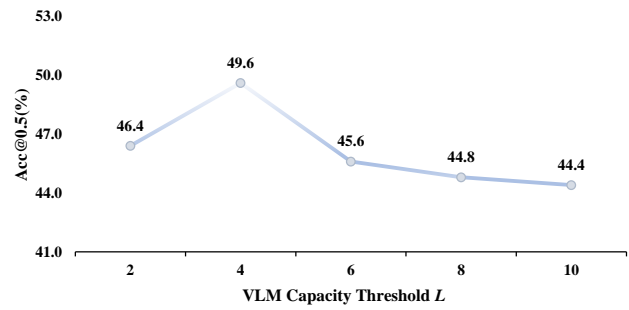


Figure 5: Ablation study on different values of batch size threshold L.



Figure 6: Ablation study on different values of multi-view frame number nframe.

cost (0.8\$). Douba-1.5-vision-pro achieves the highest accuracy (49.6 Acc@0.5) with higher token usage (7,097k), indicating superior visual-text alignment. Given the importance of precision in 3DVG, we choose Douba as the default VLM, favoring its accuracy despite increased computational cost.

Cross-Method Comparison. To decouple the impact of framework design from VLM selection, we conduct cross-method comparisons under controlled VLM settings in Table 5. When utilizing GPT-4, our SeqVLM achieves 44.0 Acc@0.5, outperforming VLM-Grounder’s 32.8 by 11.2 points, confirming fundamental architectural advantages in multimodal fusion and geometric reasoning. Simultaneously, under the Doubao VLM environment, SeqVLM attains 49.6 Acc@0.5, outperforming ZSVG3D’s 29.2 and SeeGround’s 40.0 by 20.4 and 9.6 points, respectively. These consistent superiority patterns across heterogeneous VLM backends demonstrate that our framework’s innovations in proposal selection, proposal-guided multi-view projection, and iterative reasoning constitute the primary driver of performance gains, rather than mere VLM capability differences. The results establish SeqVLM as a generalized architectural advancement for zero-shot 3D grounding, transferable across modern VLMs.

Hyper-parameter Analysis Our ablation reveals that both the VLM capacity threshold L and multi-view frame number n_{frame} exhibit inverse U-shaped effects on accuracy, peaking at $L = 4$ and $n_{frame} = 5$ (Figures 5-6). Smaller capacity threshold ($L = 2$) limit cross-candidate contrast through insufficient batch diversity, while larger capacity threshold ($L \geq 6$) overload the VLM’s multimodal reasoning. Similarly for, fewer views ($n_{frame} \leq 4$) restrict spatial disambiguation and feature richness, whereas excessive views ($n_{frame} \geq 6$) introduce redundant or occluded projections as cross-modal noise. The chosen setting ($L = 4$, $n_{frame} = 5$) provides the best trade-off between information completeness and computational load, maximizing alignment within VLM capacity.

5 Conclusion

In this paper, we propose SeqVLM, a novel framework for zero-shot 3D visual grounding that leverages multi-view real-world scene images. Our approach first employs a Proposal Selection Module to eliminate semantically irrelevant proposals, improving both reasoning accuracy and efficiency. Then, we introduce a proposal-guided multi-view projection strategy to mitigate projection misalignment and enrich contextual information across different viewpoints. To enhance the reasoning capabilities of the VLM, we further design an iterative reasoning mechanism. Evaluations on ScanRefer and Nr3D benchmarks demonstrate that SeqVLM achieves state-of-the-art performance in zero-shot 3D visual grounding, matching the accuracy of supervised approaches while requiring no task-specific training.

Acknowledgments

This work was supported in part by the National Natural Science Foundation of China under Grant 62176224, Grant 62176092, Grant 62222602, and Grant 62306165; in part by Science and Technology on Sonar Laboratory under grant 2024-JCJQ-LB-32/07 and in part by China Academy of Railway Sciences under Grant 2023Y1357.

References

- [1] Panos Achlioptas, Ahmed Abdelreheem, Fei Xia, Mohamed Elhoseiny, and Leonidas Guibas. Referit3d: Neural listeners for fine-grained 3d object identification in real-world scenes. In *European Conference on Computer Vision*, pages 422–440. Springer, 2020.
- [2] Alibaba Cloud. Tongyi Qianwen. <https://bailian.console.aliyun.com/>, 2025. Accessed: 2025-03-03.
- [3] ByteDance. VolcEngine. <https://console.volcengine.com/>, 2025. Accessed: 2025-02-18.
- [4] Daigang Cai, Lichen Zhao, Jing Zhang, Lu Sheng, and Dong Xu. 3djcg: A unified framework for joint dense captioning and visual grounding on 3d point clouds. In *Proceedings of the IEEE/CVF Conference on Computer Vision and Pattern Recognition*, pages 16464–16473, 2022.
- [5] Ziyi Cao, Tiansong Li, Shaoguo Cui, Kejun Wu, Yan Chen, Longwei Zhong, Hongkui Wang, and Li Yu. Tparn: A network for enhancing synthetic video quality after 3d-heve encoding. In *2024 IEEE International Symposium on Circuits and Systems (ISCAS)*, pages 1–5. IEEE, 2024.
- [6] Dave Zhenyu Chen, Angel X Chang, and Matthias Nießner. Scanrefer: 3d object localization in rgb-d scans using natural language. In *European Conference on Computer Vision*, pages 202–221. Springer, 2020.
- [7] Dave Zhenyu Chen, Qirui Wu, Matthias Nießner, and Angel X Chang. D 3 net: A unified speaker-listener architecture for 3d dense captioning and visual grounding. In *European Conference on Computer Vision*, pages 487–505. Springer, 2022.
- [8] Jun Chen, Deyao Zhu, Xiaoqian Shen, Xiang Li, Zechun Liu, Pengchuan Zhang, Raghuraman Krishnamoorthi, Vikas Chandra, Yunyang Xiong, and Mohamed Elhoseiny. Minigpt-v2: large language model as a unified interface for vision-language multi-task learning. *arXiv preprint arXiv:2310.09478*, 2023.
- [9] Tianrun Chen, Chunran Yu, Jing Li, Jianqi Zhang, Lanyun Zhu, Deyi Ji, Yong Zhang, Ying Zang, Zejian Li, and Lingyun Sun. Reasoning3d-grounding and reasoning in 3d: Fine-grained zero-shot open-vocabulary 3d reasoning part segmentation via large vision-language models. *arXiv preprint arXiv:2405.19326*, 2024.
- [10] Matt Deitke, Dustin Schwenk, Jordi Salvador, Luca Weihs, Oscar Michel, Eli VanderBilt, Ludwig Schmidt, Kiana Ehsani, Aniruddha Kembhavi, and Ali Farhadi. Objaverse: A universe of annotated 3d objects. In *Proceedings of the IEEE/CVF Conference on Computer Vision and Pattern Recognition*, pages 13142–13153, 2023.
- [11] Jiaru Hu, Xianhao Chen, Boyin Feng, Guanglin Li, Liangjing Yang, Hujun Bao, Guofeng Zhang, and Zhaopeng Cui. Cg-slam: Efficient dense rgb-d slam in a consistent uncertainty-aware 3d gaussian field. In *European Conference on Computer Vision*, pages 93–112. Springer, 2024.
- [12] Huajian Huang, Longwei Li, Hui Cheng, and Sai-Kit Yeung. Photo-slam: Real-time simultaneous localization and photorealistic mapping for monocular stereo and rgb-d cameras. In *Proceedings of the IEEE/CVF Conference on Computer Vision and Pattern Recognition*, pages 21584–21593, 2024.
- [13] Kuan-Chih Huang, Xiangtai Li, Lu Qi, Shuicong Yan, and Ming-Hsuan Yang. Reason3d: Searching and reasoning 3d segmentation via large language model. In *International Conference on 3D Vision 2025*, 2025.
- [14] Pin-Hao Huang, Han-Hung Lee, Hwann-Tzong Chen, and Tyng-Luh Liu. Text-guided graph neural networks for referring 3d instance segmentation. In *AAAI*, volume 35, pages 1610–1618, 2021.
- [15] Rui Huang, Henry Zheng, Yan Wang, Zhuofan Xia, Marco Pavone, and Gao Huang. Training an open-vocabulary monocular 3d detection model without 3d data. *Advances in Neural Information Processing Systems*, 37:72145–72169, 2024.
- [16] Shijia Huang, Yilun Chen, Jiaya Jia, and Liwei Wang. Multi-view transformer for 3d visual grounding. In *Proceedings of the IEEE/CVF Conference on Computer Vision and Pattern Recognition*, pages 15524–15533, 2022.
- [17] Sihwan Hwang, Sanmin Kim, Youngsook Kim, and Dongsuk Kum. Joint semi-supervised and active learning via 3d consistency for 3d object detection. In *2023 IEEE International Conference on Robotics and Automation (ICRA)*, pages 4819–4825. IEEE, 2023.
- [18] Ayush Jain, Nikolaos Gkanatsios, Ishita Mediratta, and Katerina Fragkiadaki. Bottom up top down detection transformers for language grounding in images and point clouds. In *European Conference on Computer Vision*, pages 417–433. Springer, 2022.
- [19] Sajid Javed, Arif Mahmood, Iyyakutti Iyappan Ganapathi, Fayaz Ali Dharejo, Naoufel Werghi, and Mohammed Bennamoun. Cplip: zero-shot learning for histopathology with comprehensive vision-language alignment. In *Proceedings of the IEEE/CVF Conference on Computer Vision and Pattern Recognition*, pages 11450–11459, 2024.
- [20] Li Jiang, Hengshuang Zhao, Shaoshuai Shi, Shu Liu, Chi-Wing Fu, and Jiaya Jia. Pointgroup: Dual-set point grouping for 3d instance segmentation. In *Proceedings of the IEEE/CVF Conference on Computer Vision and Pattern Recognition*, pages 4867–4876, 2020.
- [21] Justin Kerr, Chung Min Kim, Ken Goldberg, Angjoo Kanazawa, and Matthew Tancik. Lerp: Language embedded radiance fields. In *Proceedings of the IEEE/CVF International Conference on Computer Vision*, pages 19729–19739, 2023.
- [22] Jianfeng Li, Juan Dai, Zhong Su, and Cui Zhu. Rgb-d based visual slam algorithm for indoor crowd environment. *Journal of Intelligent & Robotic Systems*, 110(1):27, 2024.
- [23] Junnan Li, Dongxu Li, Silvio Savarese, and Steven Hoi. Blip-2: Bootstrapping language-image pre-training with frozen image encoders and large language models. In *International Conference on Machine Learning*, pages 19730–19742. PMLR, 2023.
- [24] Rong Li, Shijie Li, Lingdong Kong, Xulei Yang, and Junwei Liang. Seeground: See and ground for zero-shot open-vocabulary 3d visual grounding. *arXiv preprint*

arXiv:2412.04383, 2024.

[25] Jinpeng Lin, Zhihao Liang, Shengheng Deng, Lile Cai, Tao Jiang, Tianrui Li, Kui Jia, and Xun Xu. Exploring diversity-based active learning for 3d object detection in autonomous driving. *IEEE Transactions on Intelligent Transportation Systems*, 2024.

[26] Qi Liu, Yongyi He, Tong Xu, Defu Lian, Che Liu, Zhi Zheng, and Enhong Chen. Unimel: A unified framework for multimodal entity linking with large language models. In *Proceedings of the 33rd ACM International Conference on Information and Knowledge Management*, pages 1909–1919, 2024.

[27] Yang Liu, Weixing Chen, Yongjie Bai, Xiaodan Liang, Guanbin Li, Wen Gao, and Liang Lin. Aligning cyber space with physical world: A comprehensive survey on embodied ai. *arXiv preprint arXiv:2407.06886*, 2024.

[28] Ze Liu, Zheng Zhang, Yue Cao, Han Hu, and Xin Tong. Group-free 3d object detection via transformers. In *Proceedings of the IEEE/CVF International Conference on Computer Vision*, pages 2949–2958, 2021.

[29] Junyu Luo, Jiahui Fu, Xianghao Kong, Chen Gao, Haibing Ren, Hao Shen, Huaxia Xia, and Si Liu. 3d-sps: Single-stage 3d visual grounding via referred point progressive selection. In *Proceedings of the IEEE/CVF Conference on Computer Vision and Pattern Recognition*, pages 16454–16463, 2022.

[30] Kristian Micko and Peter Papcun. Motion detection methods applied on rgb-d images for vehicle classification on the edge computing. *IEEE Internet of Things Journal*, 2025.

[31] OpenAI. ChatGPT. <https://chatgpt.com/>, 2024. Version: 2024-05-13.

[32] Songyou Peng, Kyle Genova, Chiyu Jiang, Andrea Tagliasacchi, Marc Pollefeys, Thomas Funkhouser, et al. Openscene: 3d scene understanding with open vocabularies. In *Proceedings of the IEEE/CVF Conference on Computer Vision and Pattern Recognition*, pages 815–824, 2023.

[33] Thinh Phan, Khoa Vo, Duy Le, Gianfranco Doretto, Donald Adjeroh, and Ngan Le. Zeetad: Adapting pretrained vision-language model for zero-shot end-to-end temporal action detection. In *Proceedings of the IEEE/CVF Winter Conference on Applications of Computer Vision*, pages 7046–7055, 2024.

[34] Zhipeng Qian, Yiwei Ma, Zhekai Lin, Jiayi Ji, and Xiawu Zheng. Multi-branch collaborative learning network for 3d visual grounding.

[35] Xin Qiao, Matteo Poggi, Pengchao Deng, Hao Wei, Chenyang Ge, and Stefano Mattoccia. Rgb guided 3d imaging system: a survey of deep learning-based methods. *International Journal of Computer Vision*, 132(11):4954–4991, 2024.

[36] Alec Radford, Jong Wook Kim, Chris Hallacy, Aditya Ramesh, Gabriel Goh, Sandhini Agarwal, Girish Sastry, Amanda Askell, Pamela Mishkin, Jack Clark, et al. Learning transferable visual models from natural language supervision. In *International Conference on Machine Learning*, pages 8748–8763. PMLR, 2021.

[37] Jonas Schult, Francis Engelmann, Alexander Hermans, Or Litany, Siyu Tang, and Bastian Leibe. Mask3d: Mask transformer for 3d semantic instance segmentation. In *2023 IEEE International Conference on Robotics and Automation (ICRA)*, pages 8216–8223. IEEE, 2023.

[38] Ju Shen and Sen-Ching S Cheung. Layer depth denoising and completion for structured-light rgb-d cameras. In *Proceedings of the IEEE conference on Computer Vision and Pattern Recognition*, pages 1187–1194, 2013.

[39] Cameron Smith, Yilun Du, Ayush Tewari, and Vincent Sitzmann. Flowcam: Training generalizable 3d radiance fields without camera poses via pixel-aligned scene flow. *arXiv preprint arXiv:2306.00180*, 2023.

[40] Ozan Unal, Christos Sakaridis, Suman Saha, and Luc Van Gool. Four ways to improve verbo-visual fusion for dense 3d visual grounding. In *European Conference on Computer Vision*, pages 196–213. Springer, 2024.

[41] Thang Vu, Kookhoi Kim, Tung M Luu, Thanh Nguyen, and Chang D Yoo. Soft-group for 3d instance segmentation on point clouds. In *Proceedings of the IEEE/CVF Conference on Computer Vision and Pattern Recognition*, pages 2708–2717, 2022.

[42] Lei Wang, Chen Ma, Xueyang Feng, Zeyu Zhang, Hao Yang, Jingsen Zhang, Zhiyuan Chen, Jiakai Tang, Xu Chen, Yankai Lin, et al. A survey on large language model based autonomous agents. *Frontiers of Computer Science*, 18(6):186345, 2024.

[43] Yuan Wang, Yali Li, and Shengjin Wang. G⁺3-lq: Marrying hyperbolic alignment with explicit semantic-geometric modeling for 3d visual grounding. In *Proceedings of the IEEE/CVF Conference on Computer Vision and Pattern Recognition*, pages 13917–13926, 2024.

[44] Zehan Wang, Haifeng Huang, Yang Zhao, Ziang Zhang, and Zhou Zhao. Chat-3d: Data-efficiently tuning large language model for universal dialogue of 3d scenes. *arXiv preprint arXiv:2308.08769*, 2023.

[45] Jiannan Wu, Muyan Zhong, Sen Xing, Zeqiang Lai, Zhaoyang Liu, Zhe Chen, Wenhui Wang, Xizhou Zhu, Lewei Lu, Tong Lu, et al. Visionllm v2: An end-to-end generalist multimodal large language model for hundreds of vision-language tasks. *Advances in Neural Information Processing Systems*, 37:69925–69975, 2024.

[46] Yanmin Wu, Xinhua Cheng, Renrui Zhang, Zesen Cheng, and Jian Zhang. Eda: Explicit text-decoupling and dense alignment for 3d visual grounding. In *Proceedings of the IEEE/CVF Conference on Computer Vision and Pattern Recognition*, pages 19231–19242, 2023.

[47] Jie Xu, Wenlu Yu, Song Huang, Shenghai Yuan, Lijun Zhao, Ruifeng Li, and Lihua Xie. M-divo: Multiple tof rgb-d cameras enhanced depth-inertial-visual odometry. *IEEE Internet of Things Journal*, 2024.

[48] Runsen Xu, Zhwei Huang, Tai Wang, Yilun Chen, Jiangmiao Pang, and Dahu Lin. Vlm-grounder: A vlm agent for zero-shot 3d visual grounding. *arXiv preprint arXiv:2410.13860*, 2024.

[49] Zhiwen Yan, Weng Fei Low, Yu Chen, and Gim Hee Lee. Multi-scale 3d gaussian splatting for anti-aliased rendering. In *Proceedings of the IEEE/CVF Conference on Computer Vision and Pattern Recognition*, pages 20923–20931, 2024.

[50] Jianing Yang, Xuwei Chen, Shengyi Qian, Nikhil Madaan, Madhavan Iyengar, David F Fouhey, and Joyce Chai. Llm-grounder: Open-vocabulary 3d visual grounding with large language model as an agent. In *2024 IEEE International Conference on Robotics and Automation (ICRA)*, pages 7694–7701. IEEE, 2024.

[51] Zhengyuan Yang, Songyang Zhang, Liwei Wang, and Jiebo Luo. Sat: 2d semantics assisted training for 3d visual grounding. In *Proceedings of the IEEE/CVF International Conference on Computer Vision*, pages 1856–1866, 2021.

[52] Zhihao Yuan, Jinke Ren, Chun-Mei Feng, Hengshuang Zhao, Shuguang Cui, and Zhen Li. Visual programming for zero-shot open-vocabulary 3d visual grounding. In *Proceedings of the IEEE/CVF Conference on Computer Vision and Pattern Recognition*, pages 20623–20633, 2024.

[53] Zhihao Yuan, Xu Yan, Yinghong Liao, Ruimao Zhang, Sheng Wang, Zhen Li, and Shuguang Cui. Instanceref: Cooperative holistic understanding for visual grounding on point clouds through instance multi-level contextual referring. In *Proceedings of the IEEE/CVF International Conference on Computer Vision*, pages 1791–1800, 2021.

[54] TaoLin Zhang, Sunan He, Tao Dai, Zhi Wang, Bin Chen, and Shu-Tao Xia. Vision-language pre-training with object contrastive learning for 3d scene understanding. In *AAAI*, volume 38, pages 7296–7304, 2024.

[55] Wei Zhang, Miaoxin Cai, Tong Zhang, Yin Zhuang, and Xuerui Mao. Earthgpt: A universal multi-modal large language model for multi-sensor image comprehension in remote sensing domain. *IEEE Transactions on Geoscience and Remote Sensing*, 2024.

[56] Yumin Zhang, Hongliu Li, Yajun Gao, Haoran Duan, Yawen Huang, and Yefeng Zheng. Prototype correlation matching and class-relation reasoning for few-shot medical image segmentation. *IEEE Transactions on Medical Imaging*, 2024.

[57] Yuqi Zhang, Han Luo, and Yinfie Lei. Towards clip-driven language-free 3d visual grounding via 2d-3d relational enhancement and consistency. In *Proceedings of the IEEE/CVF Conference on Computer Vision and Pattern Recognition*, pages 13063–13072, 2024.

[58] Lichen Zhao, Daigang Cai, Lu Sheng, and Dong Xu. 3dvg-transformer: Relation modeling for visual grounding on point clouds. In *Proceedings of the IEEE/CVF International Conference on Computer Vision*, pages 2928–2937, 2021.

[59] Wangbo Zhao, Yizeng Han, Jiasheng Tang, Zhikai Li, Yibing Song, Kai Wang, Zhangyang Wang, and Yang You. A stitch in time saves nine: Small vlm is a precise guidance for accelerating large vlms. *arXiv preprint arXiv:2412.03324*, 2024.

[60] Zangwei Zheng, Mingyuan Ma, Kai Wang, Ziheng Qin, Xiangyu Yue, and Yang You. Preventing zero-shot transfer degradation in continual learning of vision-language models. In *Proceedings of the IEEE/CVF International Conference on Computer Vision*, pages 19125–19136, 2023.

[61] Dingfu Zhou, Xibin Song, Jin Fang, Yuchao Dai, Hongdong Li, and Liangjun Zhang. Context-aware 3d object detection from a single image in autonomous driving. *IEEE Transactions on Intelligent Transportation Systems*, 23(10):18568–18580, 2022.